Thermophysics and Aeromechanics, *2018*, *Vol. 25*, *No. 6*

DOI: 10.1134/S0869864318060057

Effect of droplet evaporation on the flow structure and heat and mass transfer in a confined swirling gas-droplet flow downstream of a tube sudden expansion*

M.A. Pakhomov and V.I. Terekhov

Kutateladze Institute of Thermophysics SB RAS, *Novosibirsk*, *Russia*

E-mails: pakhomov@ngs.ru, terekhov@itp.nsc.ru

(*Received June 04*, *2018*; *in revised form June 22*, *2018*)

The effect of flow swirl parameter and thermophysical properties of the droplet of water, ethanol, and acetone on the structure of turbulent flow and heat transfer in a gas-droplet flow was studied numerically. To describe the dynamics and heat and mass transfer of the two-phase flow, the Eulerian approach was used. The growth of the volume fraction of small particles on the tube axis is typical of a swirling flow because of their accumulation in the zone of reverse flows due to the turbophoresis force. It is shown that the addition of droplets leads to a significant increase in heat transfer (more than 2.5 times) at mass concentration of droplets $M_{L1} = 0.1$ in comparison with a single-phase swirling flow. Intensification of heat transfer with the use of ethanol droplets is higher than that for water droplets (approximately 10–20 %) and acetone (up to 65 %). When using the droplets of ethanol and acetone, the region of two-phase flow existence reduces, and the degree of suppression of carrier phase turbulence decreases. This is due to a more rapid evaporation of droplets of volatile liquids.

Key words: gas-droplet flow, separation, swirl, evaporation, numerical simulation, turbulence, model of Reynolds stress transport.

Introduction

Flow swirl is an effective method of controlling its structure and heat and mass transfer [1–5]. It is often used in practice in separators, vortex heat and mass exchangers and other devices. Swirling flows are characterized by flow recirculation regions, large local gradients of averaged and pulsation velocities, and increased level of turbulence; they are accompanied by complex hydrodynamic phenomena arising due to the action of centrifugal and Coriolis forces [1, 2]. The swirling confined flows behind a sudden tube expansion are widely used to stabilize the combustion process in the reacting flows in industrial burners. The presence of recirculation flow caused by a sudden flow expansion has a significant effect on the processes of momentum and heat transfer, dispersed phase distribution and determines largely the structure of separated two-phase flow [6–11]. Interaction between small particles and turbulent vortices of the gas phase in separation flows after a sudden expansion of a flat channel or tube, even without flow swirl, is a complex and not fully understood process [7, 8, 11]. The thermophysical properties of liquid droplets can influence the intensity of heat transfer processes and turbulence. For different

* The work was financially supported by the grant of Russian Science Foundation (Project No. 18-19-00161).

liquids, the specific heat of phase transitions can differ significantly (for example, for water and acetone), accordingly, the evaporation rate of droplets changes, and the particle size has a significant effect on gas phase turbulence.

Over the past two decades, there were experimental (see, for example, [12]) and numerical [13–19] studies of gas-droplet swirling confined flows, including those at combustion of dispersed fuel particles [17–19]. In [17], the Eulerian model was developed and numerical results were compared with experimental results on the process of fuel droplet evaporation in a swirling gas flow. Gas phase turbulence was described using the k–ε model, which takes into account the influence of particles and carrier flow swirl. Good agreement with the measurements was obtained. In [18], a swirling gas-droplet flow in a tube in the presence of burning liquid droplets of fuel was simulated using a 3D RANS-approach. The effect of gas turbulence on the rate of droplet evaporation was shown. It was found that at swirl parameters S < 1, this effect cannot be neglected far from the inlet cross section, and at S > 1, this effect cannot be neglected also close to it. Various modifications of isotropic turbulence models are unacceptable for calculating the velocity field in the swirling confined flows. The Boussinesq hypothesis used in calculations of Reynolds stresses in isotropic models overestimates the value of their tangential component [17]. One of the methods allowing partial consideration of the complex mixing processes and anisotropy of phase velocity pulsations in two-phase separated swirling flows is the use of models of transport of the components of Reynolds stress tensor (Second-Moment Closure) [14, 15].

An important aspect of the study of turbulent two-phase flows is a possibility of controlling the turbulent kinetic energy of the gas phase. Understanding the physical mechanisms of particle interaction with carrier phase turbulence also makes it possible to control friction and heat transfer in such flows [7, 8, 10, 11]. The purpose of the present study is the numerical simulation of the effect of flow swirl on dispersed phase distribution and heat transfer in the gas-droplet flow behind a sudden tube expansion. The presented work is the development of research [14, 15], where only structure and heat transfer of a two-phase swirling flow behind a sudden tube expansion with [15] and without [14] interphase heat transfer have been simulated numerically. The focus is on the effect of thermophysical properties of the liquid phase on the parameters of carrier flow turbulence and near-wall heat transfer.

Mathematical model

We considered the problem of dynamics of a two-phase swirling turbulent gas-droplet flow in the presence of heat transfer with the pipe walls. The solution uses a system of three-dimensional Reynolds-averaged Navier–Stokes (RANS) equations written with allowance for the back effect of particles on the transport processes in gas. A schematic representation of the flow is shown in Fig. 1. The volume concentration of dispersed phase is low: $\Phi_1 = M_{L1}\rho/\rho_L < 2\cdot10^{-4}$. The effects of collisions of particles with each other can be neglected, since the particles are quite small ($d_1 < 100$ μm). Here M_{L1} is the initial mass fraction of droplets, ρ and ρ_L are the density of gas and droplets. All basic equations for both phases in the current section are written in the tensor form, although they were solved for axisymmetric flow in cylindrical coordinates. This is done solely for the purpose of recording shortness.

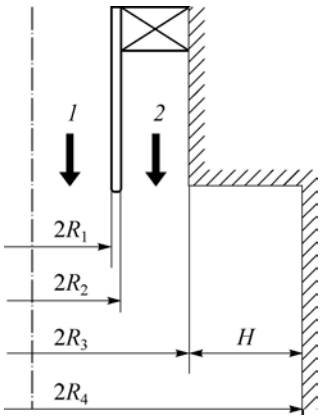

Fig. 1. Scheme of computational domain.
1 — gas-droplet nonswirling flow,
2 — single-phase swirling airflow.

System of averaged equations of gas phase

The system of three-dimensional RANS-equations, written in cylindrical coordinates with consideration of a reverse effect of particles on the processes of averaged and turbulent transfer in gas, is used here:

$$\frac{\partial\left(\rho U_j\right)}{\partial x_j}=\frac{6J}{d}\Phi,$$

$$\frac{\partial\left(\rho U_i U_j\right)}{\partial x_j}=-\frac{\partial\left(P+2k/3\right)}{\partial x_i}+\frac{\partial}{\partial x_j}\left(\mu\frac{\partial U_i}{\partial x_j}-\rho\left\langle u_i u_j\right\rangle\right)-$$

$$-\left(U_i-U_{\mathrm{L}i}\right)\Phi\rho_{\mathrm{L}}\left(\frac{1}{\tau}+\frac{6J}{\rho_{\mathrm{L}}d}\right)+S_i,$$

$$\frac{\partial\left(\rho U_j T\right)}{\partial x_j}=\frac{\partial}{\partial x_j}\left(\frac{\mu}{\mathrm{Pr}}\cdot\frac{\partial T}{\partial x_j}-\rho\left\langle u_j t\right\rangle\right)+D_{\mathrm{T}}\frac{\rho\left(C_{PV}-C_{PA}\right)}{C_P}\left(\frac{\partial K_V}{\partial x_i}\cdot\frac{\partial T}{\partial x_i}\right)-$$

$$-\frac{6\Phi}{C_P d}\left[\alpha\left(T-T_{\mathrm{L}}\right)+JL\right],$$

$$\frac{\partial\left(\rho U_j K_V\right)}{\partial x_j}=\frac{\partial}{\partial x_j}\left(\frac{\mu}{\mathrm{Sc}}\cdot\frac{\partial K_V}{\partial x_j}-\rho\left\langle u_j k_{\mathrm{V}}\right\rangle\right)+\frac{6\rho J\Phi}{d},\quad \rho=P/\left(R_{\mathrm{g}}T\right). \tag{1}$$

Hereinafter, U_i ($U_Z\equiv U$, $U_r\equiv V$, $U_\varphi\equiv W$), u'_i ($u_Z\equiv u'$, $u_r\equiv v'$, $u_\varphi\equiv w'$) are the components of averaged velocity and its pulsations, x_i is the projection on the coordinate axis, ν is the coefficient of kinematic viscosity, $2k=\left\langle u'_i u'_i\right\rangle=u'^2+v'^2+w'^2$ is the turbulent kinetic energy of the gas phase, $\tau=\rho_{\mathrm{L}}d_{\mathrm{l}}^2/\left(18\mu W\right)$ is the time of dynamic relaxation of particles, taking into account the deviation from the Stokes power law, Φ is the volumetric concentration of dispersed phase, $W=1+\mathrm{Re}_{\mathrm{L}}^{2/3}/6$, $\mathrm{Re}_{\mathrm{L}}=\left|\mathbf{U}-\mathbf{U}_{\mathrm{L}}\right|d/\nu$ is the Reynolds number of dispersed phase, J is the vapor mass flow rate from the surface of evaporating droplet, P is the pressure, S_i is the effect of flow swirl ($i=U,\ V,\ W$): $S_U=0$, $S_V=W^2/r-v'V/r^2+w'^2/r$ and $S_W=-VW/r-$ $-v'W/r^2+v'w'/r$ [20], T is the temperature, D_{T} is the coefficient of turbulent diffusion, C_P is the heat capacity of gas, α is the heat transfer coefficient of evaporating droplet, L is the specific heat of vaporization, K_{V} is the mass concentration of vapor in the binary vapor-gas mixture, R_{g} is the specific gas constant, Pr = ν/a and Sc = ν/D are the Prandtl and Schmidt numbers, respectively, a is the thermal diffusivity, D is the diffusion coefficient; indices: A is air, L is dispersed phase, T is turbulent parameter, V is water vapor.

We should note that the molar fraction of evaporated liquid is significantly less than the molar fraction of the main gas flow. All equations of system (1) are written taking into account the influence of dispersed phase presence and evaporation on the processes of momentum, heat and mass transfer in the gas flow. Turbulent thermal and diffusive flows in the gas phase are determined according to the Boussinesq hypothesis:

$$\rho\left\langle u_j t\right\rangle=-\frac{\mu_{\mathrm{T}}}{\mathrm{Pr}_{\mathrm{T}}}\cdot\frac{\partial T}{\partial x_j},\quad \rho\left\langle u_j k_{\mathrm{V}}\right\rangle=-\frac{\mu_{\mathrm{T}}}{\mathrm{Sc}_{\mathrm{T}}}\cdot\frac{\partial K_{\mathrm{V}}}{\partial x_j}.$$

It is assumed for the turbulent numbers of Prandtl and Schmidt: $\mathrm{Pr}_{\mathrm{T}}=\mathrm{Sc}_{\mathrm{T}}=0.85$.

Model of Reynolds stress transport

Turbulence of the gas phase was calculated using the elliptical model of Reynolds stress transport [21]:

$$\frac{\partial\left(U_j\left\langle u'_i\,u'_j\right\rangle\right)}{\partial x_j}=P_{ij}+\phi_{ij}-\varepsilon_{ij}+\frac{\partial}{\partial x_j}\left(\nu\delta_{ij}+\frac{C_\mu T_\mathrm{T}}{\sigma_k}\left\langle u'_i\,u'_j\right\rangle\right)\frac{\partial}{\partial x_i}\left\langle u'_i\,u'_j\right\rangle-A_\mathrm{L},$$

$$\frac{\partial\left(U_j\,\varepsilon\right)}{\partial x_j}=\frac{1}{T_\mathrm{T}}\left(C_{\varepsilon1}P_{ij}-C_{\varepsilon2}\varepsilon\right)+\frac{\partial}{\partial x_j}\left(\nu\delta_{ij}+\frac{C_\mu T_\mathrm{T}}{\sigma_\varepsilon}\cdot\frac{\partial\varepsilon}{\partial x_i}\right)-\varepsilon_\mathrm{L},\quad \beta-L_\mathrm{T}^2\nabla^2\beta=1. \qquad (2)$$

Here, P_{ij} is the intensity of energy transport from the averaged motion of the gas phase to the pulsation one; $P_2 = 0.5P_{kk}$, $T_\mathrm{T}=\max\left(k/\varepsilon,\ C_\mathrm{T}\sqrt{\nu/\varepsilon}\right)$ is turbulent time macroscale, ϕ_{ij} is the redistributing term, describing energy transfer between separate components $\left\langle u'_i\,u'_j\right\rangle$ due to pressure-deformation rate correlation, ε is the dissipation or rate of energy transfer from the large-scale vortices to the small-scale ones, β is the mixing coefficient determined from the elliptical equation and used for calculation of the redistributing term [22] (it varies from zero on the wall to one at a distance from the wall). Redistribution term is written taking into account the influence of the two-phase flow [23]. The last components in the right-hand sides of the system of equations (2) (A_L and ε_L) take into account the back effect of particles on the carrier phase due to pulsating interfacial slip [24, 25]:

$$A_\mathrm{L}=\frac{2\rho_\mathrm{L}\Phi}{\rho\tau}\left(1-f_u\right)\left\langle u_iu_i\right\rangle,\quad \varepsilon_\mathrm{L}=\frac{2\rho_\mathrm{L}\varepsilon}{\rho\tau}\left[\Phi\left(1-f_\varepsilon\right)\right], \qquad (3)$$

where f_u and f_ε are the coefficients of particle involvement into the turbulent motion of gas. The constants and functions of the turbulence model were defined in [21]: $C_{\varepsilon1} = 1.4$, $C_{\varepsilon2} = 1.85$, $C_{\varepsilon3} = 0.55$, $C_\mu = 0.22$, $\sigma_k = 1$, $\sigma_\varepsilon = 1.22$, and $C_\mathrm{T} = 6$.

System of averaged equations of dispersed phase

The system of averaged equations describing the transport processes in the dispersed medium looks like:

$$\frac{\partial\left(\rho_\mathrm{L}\Phi U_{\mathrm{L}j}\right)}{\partial x_j}=-\frac{6J\Phi}{d},$$

$$\frac{\partial\left(\rho_\mathrm{L}\Phi U_{\mathrm{L}j}U_{\mathrm{L}i}\right)}{\partial x_j}+\frac{\partial\left(\rho_\mathrm{L}\Phi\left\langle u_{\mathrm{L}i}u_{\mathrm{L}j}\right\rangle\right)}{\partial x_j}=\Phi\left(U_i-U_{\mathrm{L}i}\right)\frac{\rho_\mathrm{L}}{\tau}+\Phi\rho_\mathrm{L}g-\frac{1}{\tau}\cdot\frac{\partial\left(\rho_\mathrm{L}D_{\mathrm{L}ij}\Phi\right)}{\partial x_j}-\frac{\partial\left(\Phi P\right)}{\partial x_i},$$

$$\frac{\partial\left(\rho_\mathrm{L}\Phi U_{\mathrm{L}j}T_\mathrm{L}\right)}{\partial x_j}+\frac{\partial}{\partial x_j}\left(\rho_\mathrm{L}\Phi\left\langle\theta u_{\mathrm{L}j}\right\rangle\right)=\Phi\left(T-T_\mathrm{L}\right)\frac{\rho_\mathrm{L}}{\tau_\Theta}-\frac{1}{\tau_\Theta}\cdot\frac{\partial\left(\rho_\mathrm{L}D^\Theta_{\mathrm{L},ij}\Phi\right)}{\partial x_j}. \qquad (4)$$

Here, $D_{\mathrm{L}ij}$ and $D^\Theta_{\mathrm{L}ij}$ are the tensors of turbulent diffusion and turbulent heat transfer of the dispersed phase [24, 25], $\tau_\Theta = C_{P\mathrm{L}}\rho_\mathrm{L}d^2/\left(12\lambda Y\right)$ is the time of thermal relaxation of droplets, $Y=\left(1+0.3\,\mathrm{Re}_\mathrm{L}^{1/2}\,\mathrm{Pr}^{1/3}\right)$, $C_{P\mathrm{L}}$ and ρ_L are the heat capacity and density of droplet matter. The equations for calculating the second moments of pulsations of dispersed phase velocity $\left\langle u_{\mathrm{L}i}u_{\mathrm{L}j}\right\rangle$ are given in [24, 25]. The system of equations (1)–(4) is supplemented by

the equation of heat transfer at the interface under the condition of constant temperature along the droplet radius [10] and equation of vapor mass conservation on its evaporating surface [10].

Methods of numerical implementation

The method of numerical implementation of the Eulerian approach was described in detail in [10, 15]. All simulations were carried out on a grid of 256×80×80 ≈ 1.64 million control volumes. A further increase in their number does not significantly affect the results of numerical predictions.

The symmetry conditions are set on the pipe axis for gas and dispersed phases. The no-slip conditions are set on the wall surface for the gas phase. Boundary conditions on the wall surface for dispersed phase correspond to the conditions of «absorbing surface» [25], when droplets do not return to the flow after the contact with the wall. After depositions onto the pipe surface, the droplets are assumed to be momentarily evaporated. The inlet distributions of the gas flow parameters were specified using preliminary computations of a single-phase flow in a tube with the length of 150R, where R is the tube radius. Thus, a fully developed stabilized gas flow was observed in the inlet section. The dispersed phase was added to the airflow in the inlet section. For the dispersed phase, uniform distributions of the desired parameters over the tube cross section were used. When determining the initial values of the radial averaged phase velocities, relations for the law of rigid body rotation were used [26]:

$$V_1 = 4SU_1 r / R, \quad V_{L1} = 4S_L U_{L1} r / R,$$

$$S = \int_0^{R_3} \rho U_1 W_1 r^2 dr \Big/ R_3 \int_0^{R_3} \rho U_1^2 r dr,$$

$$S_L = \int_0^{R_3} \rho_L U_{L1} W_{L1} r^2 dr \Big/ R_3 \int_0^{R_3} \rho_L U_{L1}^2 r dr,$$

where S and S_L are the parameters of airflow and dispersed phase swirl, respectively.

The results of comparative analysis with experimental and calculated data for the swirling two-phase isothermal flows with solid particles and gas-droplet swirling flows at evaporation of liquid particles after a sudden tube (channel) expansion were published earlier in [15]. A good agreement between the calculated and measured data on the averaged and pulsating characteristics was obtained for both single-phase and two-phase turbulent flows (the maximal difference did not exceed 15 %).

Results of numerical calculations and their analysis

The swirling gas-droplet two-phase flow was investigated in a descending flow behind a sudden expansion of the tube (Fig. 1). The main flow of mixture of air and water, ethanol, and acetone (*1*) droplets is fed into the central channel ($2R_1$). The swirling single-phase airflow (*2*) enters the calculation area through an annular channel (R_3–R_2). The calculation area is defined by the following dimensions: $2R_1$ = 20 mm, $2R_2$ = 26 mm, $2R_3$ = 40 mm, $2R_4$ = 100 mm, step height is H = 30 mm. The length of the computational domain is X = 1 m. The mass-average axial velocity of the main airflow is U_{m1} = 15 m/s, its mass flow rate is G_1 = 5.65 g/s. The mass-average axial velocity and mass flow rate of air in the secondary annular jet is U_{m2} = = 20.7 m/s, and G_2 = 18 g/s. The velocity ratio of coaxial jets in calculations was assumed to be constant: $m = \rho_2 U_{m2} / \rho_1 U_{m1}$ = 1.2, and the parameter of flow swirl varied within S = 0–0.75.

The Reynolds number of the gas phase was $\mathrm{Re} = U_{m1} 2R_1/\nu = 2 \cdot 10^4$. The initial averaged axial velocity of droplets was U_{L1} = 12 m/s, initial diameter of water droplets was d_1 = 10−100 μm, their mass concentration was M_{L1} = 0–0.1. Time of particle relaxation, written taking into account deviation from the law of Stokes flow, is $\tau = \rho_L d^2/(18\rho\nu W)$ = 0.3−30 ms. The wall temperature was constant along the entire length of the calculation area and it was T_W = const = = 373 K, the inlet temperatures of air and droplets were $T_1 = T_{L1} = T_2$ = 293 K. The criterion characterizing the level of particle involvement into the gas phase motion is the Stokes number in averaged motion: Stk = τ/τ_f, τ_f is the turbulent time macroscale. It is shown in [7] that at Stk << 1, the low-inertia particles are involved into the separation motion of the gas phase, and at Stk >> 1, the dispersed phase does not participate in the recirculation motion. The dispersed phase passes through the shear flow region and almost does not penetrate into the separation zone. Thus, since there are almost no particles in the separation zone, no change in turbulence is observed in it. In [7], for the separated two-phase nonswirling flows, the following relation for the time of dispersed phase relaxation is given: $\tau_f = 5H/U_{m1}$ = 0.01 s. Then, for the conditions of these calculations, Stk = 0.03–2.6. The effects of break up and coalescence of the droplets are not taken into account because of the small number of particles. Droplets at the inlet have monodisperse distribution. However, while moving along the tube, the size of droplets changes in all coordinates due to heating and evaporation, i.e., it is a variable. We assume that the droplets deposited on the tube wall from the two-phase flow, evaporate instantly. This assumption is valid for the case of large temperature difference between the wall and droplet ($T_W - T_{WL}$) > 40 [10, 14, 15]. Simulations for nonswirling and swirling two-phase flows were carried out with equal mass flow rates of gas $(G_1 + G_2)_{S\neq 0} = G_{S=0}$ and dispersed $M_{L1,S\neq 0} = M_{L1,\,S=0}$ phases. The choice of water, ethanol, and acetone as the droplet material is explained by the large difference in the latent heat of evaporation of these three substances, which has a key effect on the evaporation rate of dispersed phase particles.

The radial profiles of averaged axial (Fig. 2*a*), radial (Fig. 2*b*) and tangential (Fig. 2*c*) gas velocity components in several cross sections (x/H = 2, 4, 6, 10 and 15) along the length of the computational domain are shown in Fig. 2 with variation of the swirl parameter. One can see a noticeable difference in distribution of air velocity in the nonswirling (*1*) and swirling (*2*, *3*) gas-droplet turbulent flows. In the case of non-swirling flow (*1*), a noticeable decrease in the air velocity is observed behind the cross section of flow attachment at x/H > 10; in addition, an extensive zone of recirculation flow is formed in the near-wall region of the cylindrical channel. The length of the separation region is $x_R/H \approx 10$; whereas a swirling flow is characterized by an approximately double reduction in the length of the flow separation region [15]. In the case of the flow swirl, most studied in this work, at S = 0.5 (*3*), the gas flow recirculation areas in the near-wall and axial parts of the tube are observed. The first is associated with flow separation behind the cross section of a sudden tube expansion; the second occurs in the axial part of the tube when the flow swirls intensively (S > 0.4), when the area of return flow appears [1–4]. All calculated profiles of the axial velocity of gas (Fig. 1*a*) have the expected maximum in the mixing layer, whose position shifts to the tube wall, except for the first cross section. The radial velocity component undergoes complex changes inside the channel and reduces and evens significantly along the cross section (see Fig. *2b*). Similar deformations occur with the tangential velocity of gas (see Fig. *2c*). The effect of particles on the averaged characteristics of the gas phase in the range studied by the authors is insignificant. The studies showed that the results presented for the gas-droplet flow with particles of water and for the two-phase flow with droplets of ethanol and acetone are qualitatively and quantitatively close.

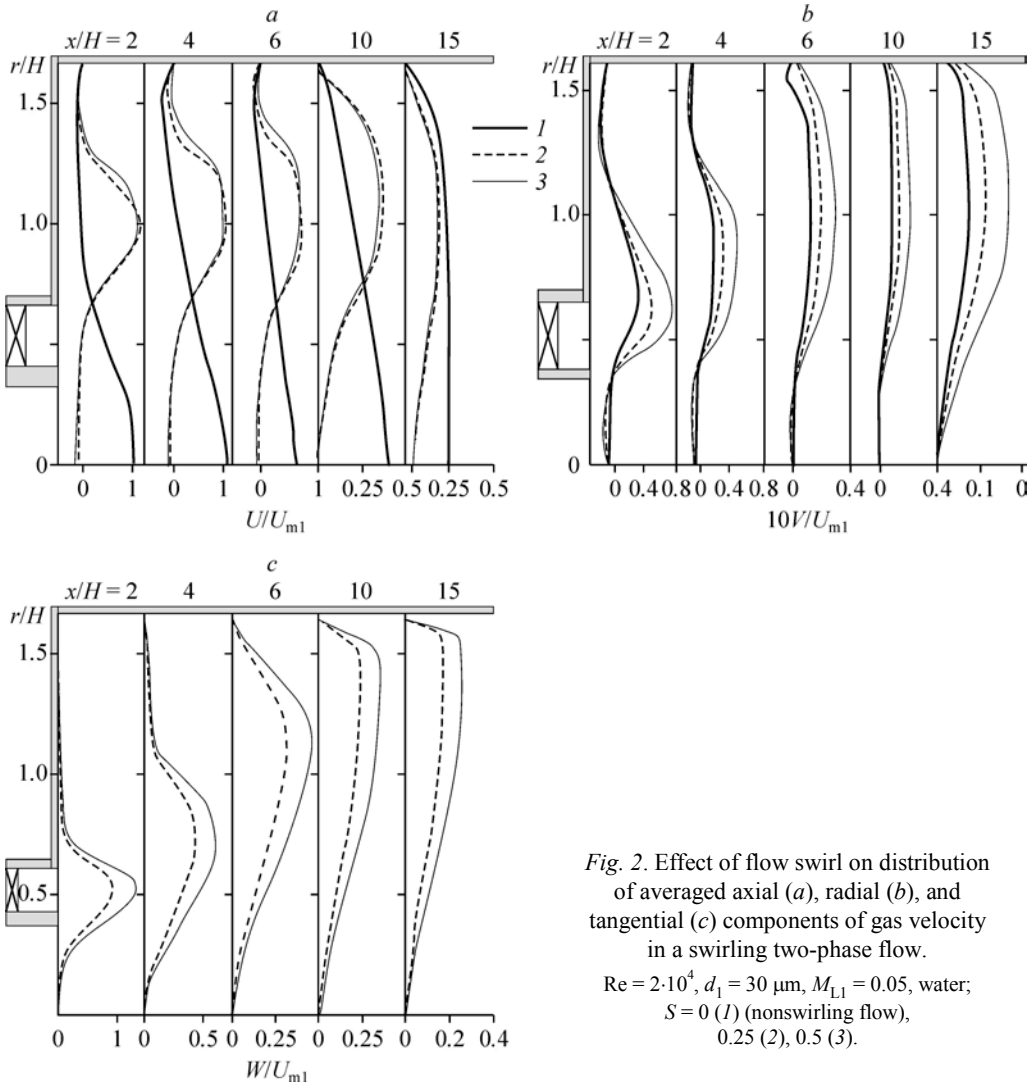

Fig. 2. Effect of flow swirl on distribution of averaged axial (*a*), radial (*b*), and tangential (*c*) components of gas velocity in a swirling two-phase flow. $\mathrm{Re} = 2 \cdot 10^4$, $d_1 = 30$ μm, $M_{L1} = 0.05$, water; $S = 0$ (*1*) (nonswirling flow), 0.25 (*2*), 0.5 (*3*).

The effect of thermophysical properties of the droplets matter on concentration profiles along the tube axis (Fig. *3a*) and in the cross section at the distance $x/H = 5$ (Fig. 3*b*) from a sudden flow expansion is presented in Fig. 3, where Φ_0 and Φ_1 are volume concentration of dispersed phase on the tube axis in the current cross section and its initial value. We should note that low-inertia droplets at small values of the Stokes number (Stk = 0.3, $d_1 = 30$ μm) are well involved into the separation flow and can be seen almost throughout the entire cross section of the tube. The near-wall part of the channel ($r/H > 1.2$) is almost free from the particles due to their intensive evaporation. In the swirling gas-droplet flow, the dispersed phase accumulates in the axial region of the jet due to the action of turbophoresis forces. The value of volume concentration of water droplets on the tube axis is maximal, and for acetone droplets, it is the lowest. This is due to a significant difference in evaporation rates of water and acetone.

Distribution of local Nusselt number along the tube length with variations in thermophysical properties of droplets (lines *1–3*) is shown in Fig. 4. Here, *4* is heat transfer in a single-phase swirling airflow and *5* is heat transfer in a stabilized flow region determined

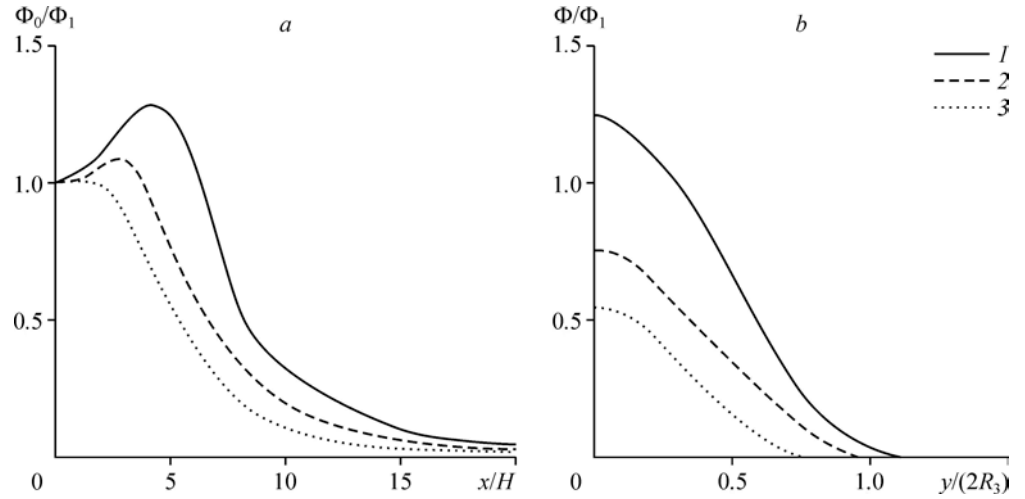

Fig. 3. Distributions of volumetric droplet concentration along the tube axis (*a*) and over its cross-section at distance $x/H = 5$ (*b*) in a swirling two-phase flow. $\mathrm{Re} = 2 \cdot 10^4$, $d_1 = 30$ μm, $M_{L1} = 0.05$, $S = 0.5$; *1* — water, *2* — ethanol, *3* — acetone.

by the parameters of a single-phase flow after a sudden pipe expansion. Adding droplets to a single-phase swirling flow leads to a noticeable increase in heat transfer intensity (more than 75 %). The highest value of heat transfer intensification is observed when ethanol drops are used, and the smallest value is observed for the acetone drops. Further, heat transfer intensity decreases, and at a large distance from the cross section of sudden expansion of the flow, heat transfer corresponds to the laws of stabilized single-phase flow in the tube. We should note that when water droplets are used as a cooler, the length of the region of intensified heat transfer is the greatest. This is explained by the fact that water has the highest amount of latent heat of vaporization, so the water droplets evaporate slower than the droplets of ethanol and acetone with all other things being equal. This is confirmed when considering the concentration profiles of liquid particles of various materials shown in Fig. 3. In a swirling flow, the position of the point of maximal heat transfer, which approximately coincides with the point of flow attachment, moves upstream. This effect increases with an increase in the swirl number, and for $S = 0.5$, the length of separation region in the swirling flow decreases almost twice in comparison with the nonswirling flow [15].

The rate of droplet evaporation, depending on the value of latent heat of evaporation, has the main influence on distribution of dispersed phase concentration, gas turbulence and heat transfer rate. Data on the effect of mass concentration of water (*1*), ethanol (*2*) and acetone (*3*) droplets

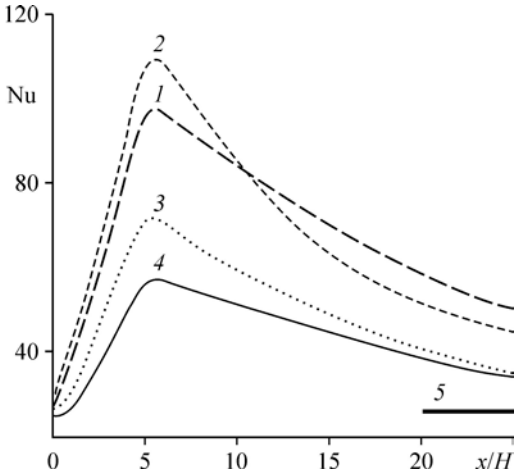

Fig. 4. Heat transfer in a swirling gas-droplet flow along the tube length with variation of droplet matter. $\mathrm{Re} = 2 \cdot 10^4$, $d_1 = 30$ μm, $M_{L1} = 0.05$, $S = 0.5$; *1* — water, *2* — ethanol, *3* — acetone, *4* — single-phase swirling airflow, *5* — heat transfer along the fully developed tube region in a single-phase airflow ($S = 0$).

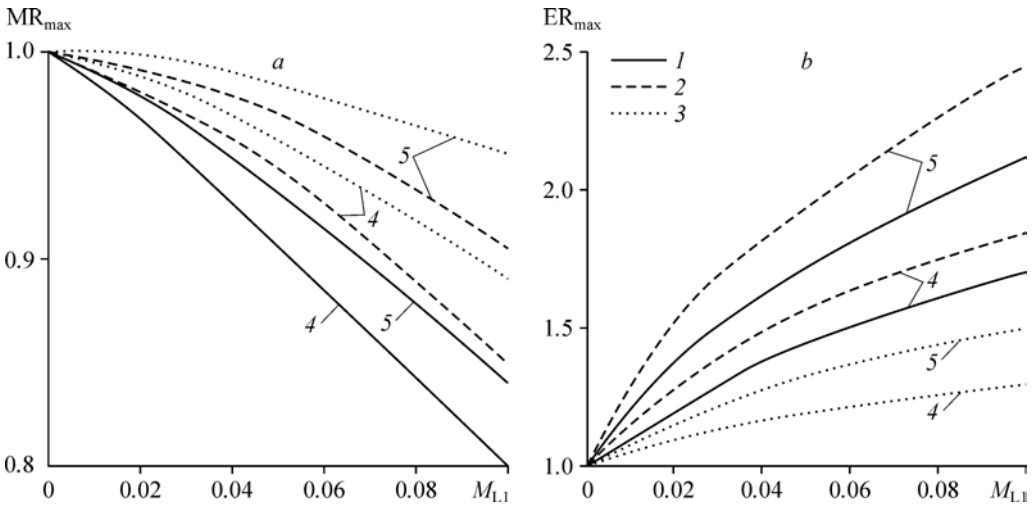

Fig. 5. Effect of thermophysical properties of liquid droplets on a change in gas turbulence $\mathrm{MR}_{max} = (k_S/k_{S,0})_{max}$ (*a*) and parameter of heat transfer intensification $\mathrm{ER}_{max} = (\mathrm{Nu}_S/\mathrm{Nu}_{S,0})_{max}$ (*b*) with variation of droplet mass concentration.

$\mathrm{Re} = 2\cdot10^4$, $d_1 = 30$ μm, $M_{L1} = 0.05$; *1* — water, *2* — ethanol, *3* — acetone, $S = 0.25$ (*4*), 0.5 (*5*).

on the maximal values of modification of gas phase turbulence MR_{max} and heat transfer intensification ER_{max} in a swirling gas-droplet flow are shown in Fig. 5. Here, $\mathrm{MR}_{max} = (k_S/k_{S,0})_{max}$ and $\mathrm{ER}_{max} = (\mathrm{Nu}_S/\mathrm{Nu}_{S,0})_{max}$, where $k = \langle u_i u_i \rangle / 2$ is turbulent kinetic energy of the carrying flow, Nu is the Nusselt number; subscript "S" corresponds to swirling flow and "0" corresponds to the single-phase airflow. An increase in the amount of the dispersed phase leads to a decrease in the level of turbulence in the two-phase flow to 20 % at $M_{L1} = 0.1$ due to involvement of the fine phase into the turbulent motion of gas. This agrees with data of [10] for the gas-dispersed turbulent flow in a vertical tube. The use of ethanol as a coolant has a smaller effect on the intensity of gas phase turbulence in comparison with the corresponding value for water droplets (to 10 %). This is due to faster heating and evaporation of ethyl alcohol droplets. Evaporation of water or ethanol droplets leads to a significant increase in heat transfer intensity in a swirling two-phase flow in comparison with a single-phase swirling flow under other identical conditions. It is shown that the addition of evaporating water and ethanol droplets leads to a significant increase in heat transfer (up to 2.5 times) in comparison with a single-phase swirling flow. Initially, there is a sharp increase in heat transfer with increasing initial mass concentration of particles. Intensification of heat transfer at using ethanol is higher than that for water droplets (approximately by 10–20 %). It should be noted that when using ethanol as a coolant, the region of two-phase flow existence decreases markedly. The droplets of acetone, which has the lowest value of the heat of phase transition, evaporate much faster than droplets of water and ethanol. Accordingly, the effect of these particles evaporation on heat transfer and turbulence of the carrier gas phase will be minimal.

Conclusion

The effect of flow swirl numbers and thermophysical properties of the droplet matter on turbulent flow structure and heat transfer in a swirling turbulent gas-droplet flow downstream of a sudden tube expansion was simulated numerically using the Eulerian approach.

The presence of two recirculation regions in the swirling flow is shown: the first region is located in the axial part of the tube; it is formed by rotation of the flow; the second region is located in the near-wall part of the pipe, and its formation is caused by separation of the flow and its further attachment. Droplets in the axial separation region cannot leave it because the level of turbulence in the shear layer is higher than that of the dispersed phase. Concentration of small particles on the tube axis is typical of a swirling flow due to their accumulation in the zone of reverse flows and action of turbophoresis force. It is shown that the addition of evaporating water and ethanol droplets into the two-phase flow leads to a significant increase in heat transfer (up to 2.5 times) in comparison with a single-phase swirling flow. Intensification of heat transfer when using ethanol droplets is higher than the corresponding value for water droplets (approximately by 10–20 %). The region of the two-phase flow and degree of turbulence suppression in the carrier phase are significantly reduced due to the presence of dispersed particles (up to 10–15 %) because of their faster evaporation. Evaporation of acetone particles with the lowest heat of phase transition has a minimal effect on heat transfer and turbulence of the carrier gas phase.

References

1. **S.S. Kutateladze, E.P. Volchkov, and V.I. Terekhov,** Aerodynamics and Heat and Mass Transfer in Confined Vortex Flows, IT SB AS USSR, Novosibirsk, 1987.
2. **V.K. Schukin and A.A. Khalatov,** Heat Transfer, Mass Transfer and Hydrodynamics of Swirling Flows in Axisymmetric Channels, Mashinostroenie, Moscow, 1982.
3. **A. Gupta, D. Lilley, and N. Syred,** Swirl Flows, Abacus Press, Tunbridge Wells, 1984.
4. **A.A. Khalatov, A.A. Avramenko, and I.V. Shevchuk,** Heat Transfer and Hydrodynamics in the Fields of Centrifugal Mass Forces. Vol. 1. Curvilinear flows, ITTF NASU, Kiev, 1996.
5. **S.V. Alekseenko and V.L. Okulov,** Swirl flow in technical applications (review), Thermophysics and Aeromechanics, 1996, Vol. 3, No. 2, P. 97–122.
6. **K. Hishida, T. Nagayasu, and M. Maeda,** Augmentation of convective heat transfer by an effective utilization of droplet inertia, Int. J. Heat Mass Transfer, 1995, Vol. 38, P. 1773–1785.
7. **J.R. Fessler and J.K. Eaton,** Turbulence modification by particles in a backward-facing step flow, J. Fluid Mech., 1999, Vol. 314, P. 97–117.
8. **F. Li, H. Qi, and C.F. You,** Phase Doppler anemometry measurements and analysis of turbulence modulation in dilute gas–solid two-phase shear flows, J. Fluid Mech., 2010, Vol. 663, P. 434–455.
9. **I. Senaha, Y. Miyafuji, S. Kato, M. Higa, and M. Yaga,** Enhancement of heat transfer in the downstream region of a backward-facing step using a small amount of mist (1st report; Study of heat transfer enhancement), (2nd report; Characteristics of heat transfer and flow behavior with mist), Trans. JSME, Pt. B, 2013, Vol. 79, P. 1816–1838.
10. **M.A. Pakhomov and V.I. Terekhov,** Second moment closure modelling of flow, turbulence and heat transfer in droplet-laden mist flow in a vertical pipe with sudden expansion, Int. J. Heat Mass Transfer, 2013, Vol. 66, P. 210–222.
11. **A.Yu. Varaksin,** Effect of particles on carrier gas flow turbulence, High Temperature, 2015, Vol. 53, No. 3, P. 423–444.
12. **L. Durdina, J. Jedelsky, and M. Jicha,** Investigation and comparison of spray characteristics of pressure-swirl atomizers for a small-sized aircraft turbine engine, Int. J. Heat Mass Transfer, 2014, Vol. 78, P. 892–900.
13. **M. Sanjose, J.M. Senoner, F. Jaegle, B. Cuenot, S. Moreau, and T. Poinsot,** Fuel injection model for Euler–Euler and Euler–Lagrange large-eddy simulations of an evaporating spray inside an aeronautical combustor, Int. J. Multiphase Flow, 2011, Vol. 37, P. 514–529.
14. **M.A. Pakhomov and V.I. Terekhov,** Solid particle spreading in gas-dispersed confined swirling flow. Eulerian and Lagrangian approaches, Thermophysics and Aeromechanics, 2017, Vol. 24, No. 3, P. 325–338.
15. **M.A. Pakhomov and V.I. Terekhov,** Numerical modeling of turbulent flow structure and heat transfer in a droplet-laden swirling flow in a pipe with a sudden expansion, Numerical Heat Transfer, Part A, 2017, Vol. 71, P. 721–736.
16. **C. Qin and E. Loth,** Numerical description of a pressure-swirl nozzle spray, Chem. Engng Proc., 2016, Vol. 107, P. 68–79.
17. **G. Klose, R. Schmehl, R. Meier, G. Maier, R. Koch, S. Wittig, M. Hettel, W. Leuckel, and N. Zarzalis,** Evaluation of advanced two-phase flow and combustion models for predicting low emission combustors, ASME J., Gas Turbines Power, 2001, Vol. 123, P. 817–823.

18. V. Sankaran and S. Menon, LES of spray combustion in swirling flows, J. Turbulence, 2002, Vol. 3, Art, No. 11, 24 p.
19. A. Sadiki, M. Chrigui, J. Janicka, and M.R. Maneshkarimi, Modeling and simulation of effects of turbulence on vaporization, mixing and combustion of liquid-fuel sprays, Flow, Turbulence Combustion, 2005, Vol. 75, P. 105–130.
20. S. Jakirlic, K. Hanjalic, and C. Tropea, Modeling rotating and swirling turbulent flows: a perpetual challenge, AIAA J., 2002, Vol. 40, P. 1984–1996.
21. A. Fadai-Ghotbi, R. Manceau, and J. Boree, Revisiting URANS computations of the backward-facing step flow using second moment closures. Influence of the numerics, Flow, Turbulence and Combustion, 2008, Vol. 81, P. 395–410.
22. R. Manceau and K. Hanjalic, Elliptic blending model: a new near-wall Reynolds-stress turbulence closure, Phys. Fluids, 2002, Vol. 14, P. 744–754.
23. N. Beishuizen, B. Naud, and D. Roekaerts, Evaluation of a modified Reynolds stress model for turbulent dispersed two-phase flows including two-way coupling, Flow, Turbulence and Combustion, 2007, Vol. 79, P. 321–341.
24. L.I. Zaichik, A statistical model of particle transport and heat transfer in turbulent shear flows, Phys. Fluids, 1999, Vol. 11, P. 1521–1534.
25. I.V. Derevich, Statistical modelling of mass transfer in turbulent two-phase dispersed flows. 1. Model development, Int. J. Heat Mass Transfer, 2000, Vol. 43, P. 3709–3723.
26. A.A. Vinberg, L.I. Zaichik, and V.A. Pershukov, Calculation of two-phase swirling flows, Fluid Dynamics, 1994, Vol. 29, No. 1, P. 55–60.